J Biol Inorg Chem (2014) 19:853–867
DOI 10.1007/s00775-014-1120-y

ORIGINAL PAPER

Anticancer activity of structurally related ruthenium(II) cyclopentadienyl complexes

Leonor Côrte-Real · Filipa Mendes · Joana Coimbra · Tânia S. Morais · Ana Isabel Tomaz · Andreia Valente · M. Helena Garcia · Isabel Santos · Manuel Bicho · Fernanda Marques

Received: 28 October 2013 / Accepted: 6 February 2014 / Published online: 23 February 2014

Abstract A set of structurally related Ru(η^5-C_5H_5) complexes with bidentate N,N′-heteroaromatic ligands have been evaluated as prospective metallodrugs, with focus on exploring the uptake and cell death mechanisms and potential cellular targets. We have extended these studies to examine the potential of these complexes to target cancer cell metabolism, the energetic-related phenotype of cancer cells. The observations that these complexes can enter cells, probably facilitated by binding to plasma transferrin, and can be retained preferentially at the membranes prompted us to explore possible membrane targets involved in cancer cell metabolism. Most malignant tumors present the Warburg effect, which consists in increasing glycolytic rates with production of lactate, even in the presence of oxygen. The reliance of glycolytic cancer cells on trans-plasma-membrane electron transport (TPMET) systems for their continued survival raises the question of their appropriateness as a target for anticancer drug development strategies. Considering the interesting findings that some anticancer drugs in clinical use are cytotoxic even without entering cells and can inhibit TPMET activity, we investigated whether redox enzyme modulation could be a potential mechanism of action of antitumor ruthenium complexes. The results from this study indicated that ruthenium complexes can inhibit lactate production and TPMET activity in a way dependent on the cancer cell aggressiveness and the concentration of the complex. Combination approaches that target cell metabolism (glycolytic inhibitors) as well as proliferation are needed to successfully cure cancer. This study supports the potential use of some of these ruthenium complexes as adjuvants of glycolytic inhibitors in the treatment of aggressive cancers.

Keywords Glycolysis · Drug targets · Redox enzymes · Cancer therapy · Ruthenium drugs

Abbreviations

AcP	Acid phosphatase
2,2′-Bipy	2,2′-Bipyridine
3BrP	3-Bromopyruvate
DCA	Dichloroacetate
2DG	2-Deoxyglucose
DTNB	Dithionitrobenzoic acid
FBS	Fetal bovine serum

L. Côrte-Real · F. Mendes · I. Santos · F. Marques (✉)
Unidade Ciências Químicas e Radiofarmacêuticas,
Instituto Superior Técnico, Universidade de Lisboa,
Polo de Loures-Campus Tecnológico e Nuclear,
Estrada Nacional 10, km 139.7,
2695-066 Bobadela LRS Sacavém, Portugal
e-mail: fmarujo@ctn.ist.utl.pt

L. Côrte-Real · T. S. Morais · A. I. Tomaz · A. Valente · M. H. Garcia
Centro de Ciências Moleculares e Materiais,
Faculdade de Ciências,,
Universidade de Lisboa,
Campo Grande, 1749-016 Lisbon, Portugal

J. Coimbra
Laboratório Central de Análises,
Universidade de Aveiro, Campus Universitário de Santiago,
3810-193 Aveiro, Portugal

M. Bicho
Laboratório de Genética, Faculdade de Medicina,
Universidade de Lisboa,
Edifício Egas Moniz, Av. Prof. Egas Moniz,
1649-028 Lisbon, Portugal

M. Bicho
Instituto Bento da Rocha Cabral,
1250-047 Lisbon, Portugal

IC_{50}	Half-maximal inhibitory concentration
ICP-MS	Inductively coupled plasma mass spectrometry
Me_2bipy	4,4′-Dimethyl-2,2′-bipyridine
mTPPMS	*m*-Diphenylphosphane benzene-3-sulfonate
MTT	3-(4,5-Dimethyl-2-thiazolyl)-2,5-diphenyltetrazolium bromide
NR	Neutral red
PAO	Phenylarsine oxide
PBS	Phosphate-buffered saline
pCMBS	*p*-Chloromercuribenzene sulfonate
pNPP	*p*-Nitrophenyl phosphate
PPh_3	Triphenylphosphane
TM34	$[Ru(\eta^5\text{-}C_5H_5)(PPh_3)(2,2'\text{-bipy})][CF_3SO_3]$
TM85	$[Ru(\eta^5\text{-}C_5H_5)$(mTPPMSNa)$(2,2'\text{-bipy})][CF_3SO_3]$
TM102	$[Ru(\eta^5\text{-}C_5H_5)(PPh_3)(Me_2bpy)[CF_3SO_3]$
TPMET	Trans-plasma-membrane electron transport
Tris	Tris(hydroxymethyl)aminomethane

Introduction

In the search for metal complexes for treatment of cancers, a broad spectrum of ruthenium compounds have been shown to exhibit potential anticancer properties, emerging as promising alternatives to platinum-based cancer therapy [1–4]. As a result of intense research focused on their cytotoxic effects and also their mechanism of action, two Ru(III) compounds, NAMI-A and KP1019, have already entered clinical trials, and a few others, in particular Ru(II)(η^6-arene) compounds, are currently undergoing preclinical evaluation [5–11].

Ruthenium complexes are thought to have a mode of action distinct from that of platinum compounds. Whereas for cisplatin, the classic platinum drug, DNA is believed to be the primary molecular target, for ruthenium complexes the targets and the exact mechanism of action are still not well understood. Their DNA-binding ability is often not absolutely related to their antitumor activities, and the interactions detected are few and weaker than for cisplatin. Other molecular targets, such as intracellular or extracellular proteins, may play the most important role in the cell death mechanisms [12–14]. Thiol-containing molecular targets including the redox enzymes thioredoxin reductase and glutathione reductase, transcription factors, and cysteine proteases such as caspases and cathepsins have been identified as alternative novel targets for these metal-based drugs [15–18].

Our search in the field of organometallic Ru(II) complexes which pioneered the family of Ru(η^5-C_5H_5) derivatives found for complexes with aromatic bidentate N,N′-heteroaromatic ligands interesting stability properties, as well as excellent cytotoxic activity against several human tumor cell lines. The extent of DNA interaction if considered alone does not correlate well with the high cytotoxic activity observed within this family of compounds, which suggests that other biological targets might be involved in the mechanism of action [19–23].

In our ongoing studies on the antitumor potential of Ru(η^5-C_5H_5) derivatives, we found for $[Ru(\eta^5\text{-}C_5H_5)(PPh_3)(2,2'\text{-bipy})][CF_3SO_3]$ (TM34)—where 2,2′-bipy is 2,2′-bipyridyl and PPh_3 is triphenylphosphane—high cytotoxic activity against human tumor cell lines, in particular A2780 ovarian cancer cells and MDA-MB-231 breast cancer cells. The results obtained for TM34 revealed fast antiproliferative effects even at short incubation times for both cell lines; preferential localization at the cell membranes (inductively coupled plasma mass spectrometry, ICP-MS); cellular uptake by an energy-dependent process, probably endocytosis; inhibition of a lysosomal enzyme, acid phosphatase (AcP), by a dose-dependent mode; and disruption and vesiculation of the Golgi apparatus (transmission electron microscopy), which suggest the endosomal/lysosomal system as a possible target [24]. A similar effect, but at a higher dose (100 μM, 3 h treatment), was found for its water-soluble analogue $[Ru(\eta^5\text{-}C_5H_5)$(mTPPMSNa)$(2,2'\text{-bipy})][CF_3SO_3]$ (TM85)—where mTPPMS is *m*-diphenylphosphane benzene-3-sulfonate—in MDA-MB-231 cells, confirming the effect of the complex on the endomembrane system [21, 24]. This result appeared to be related to the differences in the cytotoxic activity of both complexes.

In the continuing search for the "magic bullet" that will destroy both primary and metastatic cancers while exhibiting minimal toxicity, one must try novel approaches to target one or more phenotypes unique to cancer cells. The tumor energy metabolism has been proposed as a promising area for the development of anticancer drugs. Since the metabolism of cancer is different from that of healthy cells, drugs that target this metabolic difference have the potential to selectively kill cancer cells while sparing normal cells and tissues [25–27].

The challenge is to find new agents that can target one or more phenotypes unique to cancer cells. The energetic-related phenotype of cancer cells, elevated metabolism of glucose to lactic acid (glycolysis) even in the presence of oxygen [29], has been explored for the noninvasive detection and grading of tumors by positron emission tomography using the ^{18}F-labeled glucose analogue 2-deoxyglucose (2DG) [25–30]. Glycolytic enzymes and glucose transporters are overexpressed in tumor cells compared with normal cells, thus offering the opportunity for clinical investigation [28, 30–33]. Even though several components of the glycolytic pathway have been targeted

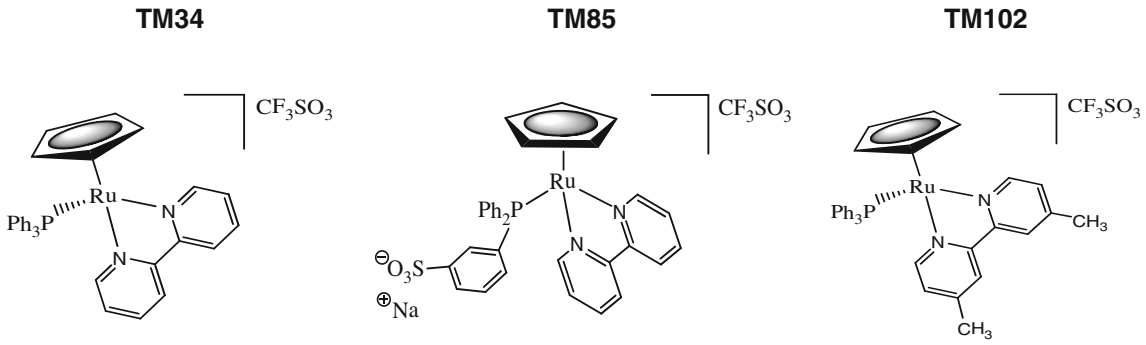

Fig. 1 Chemical structures of related Ru(η^5-C_5H_5) complexes with bidentate N,N′-heteroaromatic ligands

for therapy development, relatively few have been investigated in clinical trials. At present, the most promising therapeutic strategies use glycolytic inhibitors [e.g., 2DG, 3-bromopyruvate (3BrP), and dichloroacetate (DCA)] either alone or in combination with a chemotherapeutic agent to improve the cytotoxic efficacy [34–40].

High glycolytic rates in rapidly proliferating cells lead to a buildup of reducing equivalents (NADH) produced during glycolysis and the mitochondrial tricarboxylic acid cycle. Cells use plasma-membrane-bound oxidoreductases and enzymatic electron transfer chains to cooperate with intracellular redox pairs (e.g., pyruvate and lactate) in order to alleviate the reductive stress and maintain redox homeostasis [40–42]. Although the physiological roles are not yet completely understood, functions in which plasma membrane redox systems have been implicated are proton extrusion and control of internal pH, generation of superoxide, reduction of ferric iron and iron uptake, and control of cell growth and cell proliferation among others [43–45]. Evidence for trans-plasma-membrane electron transport (TPMET) systems is found in all cells, representing a conserved mechanism for redox regulation of cellular metabolism [44–49].

Reducing equivalents from cytosolic NADH are transported to extracellular electron acceptors through TPMET. Oxygen, dehydroascorbate, and diferric transferrin have been proposed as the physiological electron acceptors [50, 51]. When the artificial electron acceptor ferricyanide is used as the external acceptor, the system uses voltage-dependent anion channel protein 1 for transfer of electrons across the membrane from internal NADH to an external electron acceptor [52]. Ferricyanide has been commonly used to measure NADH-ferricyanide reductase activity [53–55].

The TPMET system is recognized as playing important roles in various disease states, including cancer progression [56]. The importance of TPMET in cancer cells, indicated by its increased activity in rapidly proliferating cells and the reliance of cancer cells on glycolysis for their continued survival brings about the question of its suitability as a target for anticancer drug development [57].

The challenge for novel anticancer drug strategies that target TPMET is the development of drugs that specifically locate in the plasma membrane [58].

The aim of this study was to investigate the potential of a series of Ru(η^5-C_5H_5) complexes with bidentate N,N′-heteroaromatic ligands (Fig. 1) to target cancer cell metabolism. TPMET has already been reported to be inhibited by several antitumor drugs [59, 60]. Considering the interesting findings that some of these drugs, e.g., anthracyclines (adriamycin), bleomycin, and cisplatin, are cytotoxic and inhibit NADH-ferricyanide reductase activity, some even without entering cells (adriamycin), we investigated whether this redox enzyme is inhibited by our ruthenium complexes and could be explored as a potential target for developing antitumor compounds.

Materials and methods

Chemicals and reagents

The ruthenium complexes (Fig. 1) were synthesized as previously described (TM34 [19, 23], TM85 [21], and [Ru(η^5-C_5H_5)(PPh_3)(Me_2bpy)[CF_3SO_3] (TM102)—where Me_2bpy is 4,4′-dimethyl-2,2′-bipyridine [22]) under a dinitrogen atmosphere using current Schlenk techniques.

All chemicals were of analytical or reagent grade and were used as received from chemical suppliers, unless otherwise stated. 3-(4,5-Dimethyl-2-thiazolyl)-2,5-diphenyltetrazolium bromide (MTT), human serum apotransferrin, amiloride, chloroquine, phenylarsine oxide (PAO), 2DG, 3BrP, DCA, Triton X-100, ferene-S, cisplatin, *p*-chloromercuribenzene sulfonate (pCMBS), and *p*-nitrophenyl phosphate (pNPP) were obtained from Sigma-Aldrich. Dimethyl sulfoxide and dithionitrobenzoic acid (DTNB) were purchased from Thermo Scientific. The culture media RPMI medium and Dulbecco's modified

Eagle's medium and media supplements phosphate-buffered saline (PBS), fetal bovine serum (FBS), penicillin/streptomycin, and trypsin–EDTA were obtained from Gibco, Invitrogen, Life Technologies. The Fraction-PREP™ cell fractionation kit and the lactate assay kit were purchased from BioVision (USA). The neutral red (NR)-based assay kit was purchased from Sigma-Aldrich and the DC protein assay kit was purchased from Bio-Rad.

Cell culture

Three human tumor cell lines—A2780 ovarian cancer cells and MCF7 and MDA-MB-231 breast cancer cells (ATCC)—were cultured in RPMI medium (A2780) or Dulbecco's modified Eagle's medium with GlutaMAX I (MCF7, MDA-MB-231) supplemented with 10 % (v/v) FBS and 1 % penicillin/streptomycin at 37 °C in a humidified atmosphere with 5 % CO_2. For the assays, cells in exponential growth were detached with trypsin–EDTA and suspended in fresh medium at adequate densities.

For evaluation of cellular viability, cells were seeded in 96-well plates at 10×10^3–20×10^3 cells per well and allowed to adhere for 24 h. Cells were treated with six concentrations of the ruthenium complexes previously dissolved in dimethyl sulfoxide (less than 0.5 % final concentration) in the range from 0.0 to 100 μM and incubated for 3–72 h (37 °C, 5 % CO_2). Cisplatin (the reference compound), whenever applied, was first solubilized in H_2O and then added at the same concentrations used for the ruthenium complexes.

Cellular viability assays

MTT assay

After treatment with the complexes, the medium was discarded and then MTT was added to each well (1.2 mM final concentration) for a further 3–4 h incubation at 37 °C.

The cytotoxic activity was determined by comparing the absorbance at 570 nm of the resulting solutions of the treated cells with the absorbance of the untreated cells in a multiwell plate spectrophotometer (PowerWave Xs, Bio-Tek Instruments, USA). The cytotoxic effect of the compounds was quantified by calculating the half-maximal inhibitory concentrations (IC_{50}).

AcP assay

The AcP activity was determined by a previously described method in MDA-MB-231 cells (10×10^3 cells per 200 μL medium) using 96-well plates [24]. Briefly, after treatment with the complexes for 3 h, the medium was discarded, the cells were washed with PBS, and then 100 μL of assay buffer containing 0.1 M acetate buffer pH 5.0, 0.1 % Triton X-100, and 10 mM pNPP was added. The plates were then placed in a 5 % CO_2 incubator at 37 °C for 2 h. The reaction was stopped by the addition of 10 μL of 1 M NaOH. The absorbance of *p*-nitrophenol was measured at 405 nm.

NR assay

NR assay was performed with a kit from Sigma-Aldrich. Briefly, after treatment with the complexes, cells were washed with PBS and 200 μL serum-free medium containing 0.33 % NR was added to each well. The plates were incubated at 37 °C with 5 % CO_2 for a further 3–4 h. After incubation, the plates were removed from the incubator, gently washed with NR assay fixative, and then 200 μL of NR solubilization agent was added to each well. The plates were protected from light and shaken for 10 min. The absorbance was measured in each well at 540 nm.

Cellular viability assays with complex–transferrin conjugates

The effect of the complexes binding to human serum transferrin on the cellular viability of A2780 cells was evaluated at concentrations of 0.5 μM (TM34, TM102) and 10 μM (TM85), equivalent to the IC_{50} values found for 24 h treatment. Iron-bound transferrin was prepared by loading apotransferrin with Fe(II) following a method previously described by us [61]. Briefly, solutions of protein (iron-bound transferrin) in 0.2 mL of appropriate buffer (PBS containing 25 mM Na_2CO_3, pH 7.4) were added to solutions of the ruthenium complexes (0.2 mL) in order to obtain different protein-to-ruthenium molar ratios. These solutions were allowed to form complex–protein conjugates (1.5 h at 37 °C) and were then diluted 1:10 with medium containing only 5 % FBS prior to incubation with A2780 cells. After 24 h incubation, the treatment solutions were removed and the cellular viability was measured by the MTT assay.

DNA interaction

The plasmid DNA used for gel electrophoresis experiments was ΦX174 (Promega). DNA interaction was evaluated by monitoring the mobility of the supercoiled plasmid DNA (form I) and nicked circular DNA (form II). Each reaction mixture was prepared by adding 6 μL of water, 2 μL (200 ng) of supercoiled DNA, 2 μL of 100 mM stock Na_2HPO_4/HCl pH 7.2 buffer solution, and 10 μL of the aqueous solution of the complex. The final reaction volume was 20 μL, the final buffer concentration was 10 mM, and the final metal concentration varied from 0.1 and 0.5 μM to

100 and 300 μM (depending on the complex). Samples were typically incubated for 24 h at 37 °C in the dark. After incubation, 5 μL of DNA loading buffer (0.25 % bromophenol blue, 0.25 % xylene cyanol, 30 % glycerol in water, Applichem) was added to each tube, and the sample was loaded onto a 0.8 % agarose gel in 89 mM tris(hydroxymethyl)aminomethane (Tris)–borate, 1 mM EDTA pH 8.3. Controls of nonincubated plasmid and of plasmid incubated with dimethyl sulfoxide were loaded on each gel electrophoresis. The electrophoresis was carried out for 2.5 h at 100 V. The gels were then stained with 89 mM Tris–borate, 1 mM EDTA, pH 8.3 containing ethidium bromide (0.5 μg/mL). Bands were visualized under UV light, and images were captured using an AlphaImagerEP (Alpha Innotech). All samples were obtained from the same run.

Intracellular distribution of ruthenium complexes

To explore uptake of the complex and its intracellular distribution, A2780 cells (1×10^6 cells in 5 mL medium) were exposed to each ruthenium complex at 10 μM for 3 h at 37 °C, then washed with cold PBS and centrifuged to obtain a cellular pellet following a previously described procedure [62]. Cytosol, nucleus, membrane/particulate, and cytoskeletal fractions were separated using a commercial kit (FractionPREP cell fractionation kit from BioVision) according to the manufacturer's recommendations. The ruthenium content in the different fractions was measured after digestion by a Thermo XSERIES quadrupole ICP-MS instrument (Thermo Scientific). Briefly, samples were digested with ultrapure HNO_3, H_2O_2, and HCl in a closed pressurized microwave digestion unit (Mars5, CEM) with medium-pressure HP500 vessels and then diluted in ultrapure water to obtain a 2.0 % (v/v) acid solution. The instrument was tuned using a multielement ICP-MS 71 C standard solution (Inorganic Venture). Indium-115 at 10 μg/L was used as an internal standard.

Uptake of the complex in A2780 cells was also evaluated after binding of the complex to human serum transferrin at 2:1 protein-to-ruthenium molar ratios. Complexes were tested at a concentration equivalent to the IC_{50} values found for 24 h incubation (TM34 and TM102, 0.5 μM; TM85, 10 μM).

To express metal accumulation in nanomoles per milligram of protein, the protein content in each well was quantified by a DC protein assay kit.

Effect of glycolytic inhibitors and the complexes on lactate levels

The effect of glycolytic inhibitors and the complexes on lactate levels was evaluated in MDA-MB-231 cells after a 3-h challenge. For that purpose, cells (10×10^3 per 200 μl) were seeded in 96-well plates and allowed to adhere for 24 h. Cells were starved overnight in medium without serum and then treated with the glycolytic inhibitors 2DG (20 mM), 3BrP (20 μM), and DCA (20 mM), and the ruthenium complexes TM34 (5 μM), TM85 (100 μM), and TM102 (5 μM).

All the compounds were used at noncytotoxic concentrations in cultured medium without FBS and phenol red for 3 h incubation. After incubation, cells were washed twice with PBS and lysed in buffer containing 10 mM Tris–HCl and 1 % Triton X-100 for 1 h at 37 °C. The lactate levels were determined using a colorimetric-based lactate measurement kit (BioVision) according to the manufacturer's instructions. Briefly, the cell lysate was incubated with an enzymatic mix, generating an intermediate that subsequently interacted with a probe. The absorbance was measured by a microplate spectrophotometer at 570 nm. Average data from four independent experiments (each in triplicate) were used for calculating the mean and are presented as the percent activity measured in untreated cells (± the standard deviation).

Effect of glycolytic inhibitors and their combination with the complexes on cellular viability

The effect of the glycolytic inhibitors combined with the complexes on the cellular viability of MDA-MB-231 cells was evaluated only for TM85. For that purpose, MDA-MB-231 cells were seeded in 96-well plates, incubated at 37 °C, and allowed to adhere for 24 h. Then, TM85 (1, 10, and 100 μM) was combined with the glycolytic inhibitors, namely, 2DG (20 mM), 3BrP (20 μM), and DCA (20 mM), for 24 h incubation. After the incubation, the supernatant was removed and an MTT solution was added to determine the cellular toxicity, as described earlier.

Measurement of TPMET

Ferricyanide reductase activity in MDA-MB-231 cells was determined by a colorimetric method similar to the one described by Lane and Lawen [53] using a microplate format. This method uses ferene-S as the ferrous chromogen instead of the classic bathophenanthroline sulfonate to improve the sensitivity of the assay in the determination of iron [55]. Briefly, ferricyanide reduction was performed in six-well plates containing approximately 10^6 cells per 2 mL medium without FBS and phenol red. Ferricyanide reduction was initiated after 15 min preincubation with $Ru(\eta^5\text{-}C_5H_5)(PPh_3)_2Cl$, $Ru(\eta^5\text{-}C_5H_5)(mTPPMSNa)_2Cl$ (10 μM), TM34, TM85, cisplatin (10 μM), TM102 (0.1 μM), PAO, DTNB (10 μM), and pCMBS, amiloride, chloroquine, and 2DG (1 mM) by addition of ferricyanide

(20 μL, 100 mM). Thereafter, cells were incubated for a further 20 min. Aliquots (100 μL) were taken from the wells for ferrocyanide analysis. For ferrocyanide determination, the following working solutions were prepared: solution A, 3 M sodium acetate, adjusted to pH 6.0 with acetic acid; solution B, 0.2 M citric acid; solution C, 3.3 mM ferric chloride in 0.1 M acetic acid; and solution D, 40 mM ferene-S. In a typical experiment, 100 μL of the sample were added to wells in a 96-well plate and then acidified with 10 μL acetic acid (7.7 % v/v). Ferene-S developer solution was prepared immediately before use by combining solutions A–C in a 2:2:2 volume ratio and was added (100 μL) to the sample. Then, 50 μL of solution D was then added to each sample (final volume 260 μL). The plates were agitated at room temperature for 30 min in the dark. The absorbance was measured at 620 nm with a microplate spectrophotometer. Ferrocyanide concentration was obtained as nanomoles of ferrocyanide per minute per milligram of protein using 33.2/mM/cm as the extinction coefficient for ferene-S. All values were corrected for background readings of cells with compounds in the presence of ferricyanide immediately after initiation of the assay ("time zero").

Results

Cytotoxic activity in human tumor cell lines

MTT assay

The cytotoxic activity of the complexes was evaluated by the MTT cellular viability assay in order to detect any possible structure–activity relationship and any differences between the three cell lines regarding their sensitivity to the compounds. This assay is based on the conversion of the water-soluble tetrazolium salt MTT to its insoluble purple formazan by a mitochondrial oxidoreductase. By the MTT assay, cellular viability is a measure of the metabolic activity of living cells [63]. For this purpose, three human tumor cell lines were used: A2780 ovarian cancer cancer cells, sensitive to cisplatin; MCF7 estrogen receptor positive (ER+) breast cancer cells; and MDA-MB-231 triple-negative (estrogen receptor negative, progesterone receptor negative, no HER2 overexpression) breast cancer cells. The effect of the complexes on the cellular viability was evaluated within the concentration range from 0.1 nM to 100 μM after different exposure times: 3, 24, 48, and 72 h. The IC_{50} values were calculated for each compound and cell line as shown in Table 1 and Fig. 2. The order of potency observed was TM102 > TM34 ≫ TM85. The leader complex, TM34, exhibited high anticancer activities in the micromolar range at shorter incubation times [23, 24]. Its water-soluble analogue, TM85, was found to be less active [21]. Changes in the bipyridyl ligand with the introduction of methyl groups (TM102) resulted in a complex with slightly improved cytotoxic activity when compared with its parental complex [22]. The IC_{50} values found for the ruthenium complexes after a 3-h challenge were in the ranges from 6 to 40 μM, from 11 μM to more than 200 μM, and from 20 μM to more than 200 μM for the A2780, MCF7, and MDA-MB-231 cell lines, respectively (Table 1, Fig. 2). All the complexes display higher antitumor activities against the ovarian cisplatin-sensitive cancer cells at short incubation times, although TM85 was the least effective complex. After 3 h treatment, TM85 also exhibited lower cytotoxic activity against the breast cancer cells.

Table 1 Half-maximal inhibitory concentrations (IC_{50}) of the ruthenium complexes with regard to A2780, MCF7, and MDA-MB-231 cells after 3 h incubation

Complex	IC_{50} (μM)		
	A2780	MCF7	MDA-MB-231
TM34	12.5 ± 3.50	17.3 ± 3.9	24.5 ± 11.3
TM85	40.2 ± 22.8	>200 μM	>200 μM
TM102	5.89 ± 1.71	10.9 ± 4.20	20.5 ± 8.16

See Fig. 1 for the structures of the complexes.

The cytotoxic effect of the precursors and the ligands was also evaluated in A2780 cells after 72 h exposure. In these conditions, the IC_{50} values found were 41.9 ± 16, 25.1 ± 8.5, 79.4 ± 13.5, and 76.6 ± 19 μM for $Ru(\eta^5\text{-}C_5H_5)(PPh_3)_2Cl$, $Ru(\eta^5\text{-}C_5H_5)(mTPPMSNa)_2Cl$, 2,2′-bipy, and Me_2bipy, respectively, which indicate that coordination to the ligands (2,2′-bipy or Me_2bipy) led to an enhancement of the cytotoxic potencies by at least two orders of magnitude.

AcP and NR assays

In addition to the MTT assay, assays based on different principles were used to measure cytotoxicity for comparison and eventually to detect early cytotoxic events induced by the complexes. AcP assay is based on the ability of the enzyme AcP in lysosomes to catalyze the hydrolysis of pNPP to *p*-nitrophenol at acidic pH [64]. AcP was measured to evaluate trapping of the complexes in lysosomes, as the complexes are cationic, and their effect on the lysosomal activity [24]. NR assay is based on the incorporation and binding of NR, a weak cationic dye, in the lysosomes of viable cells. Accordingly, cellular viability is a measure of lysosomal activity (AcP) and integrity (NR) [24, 63].

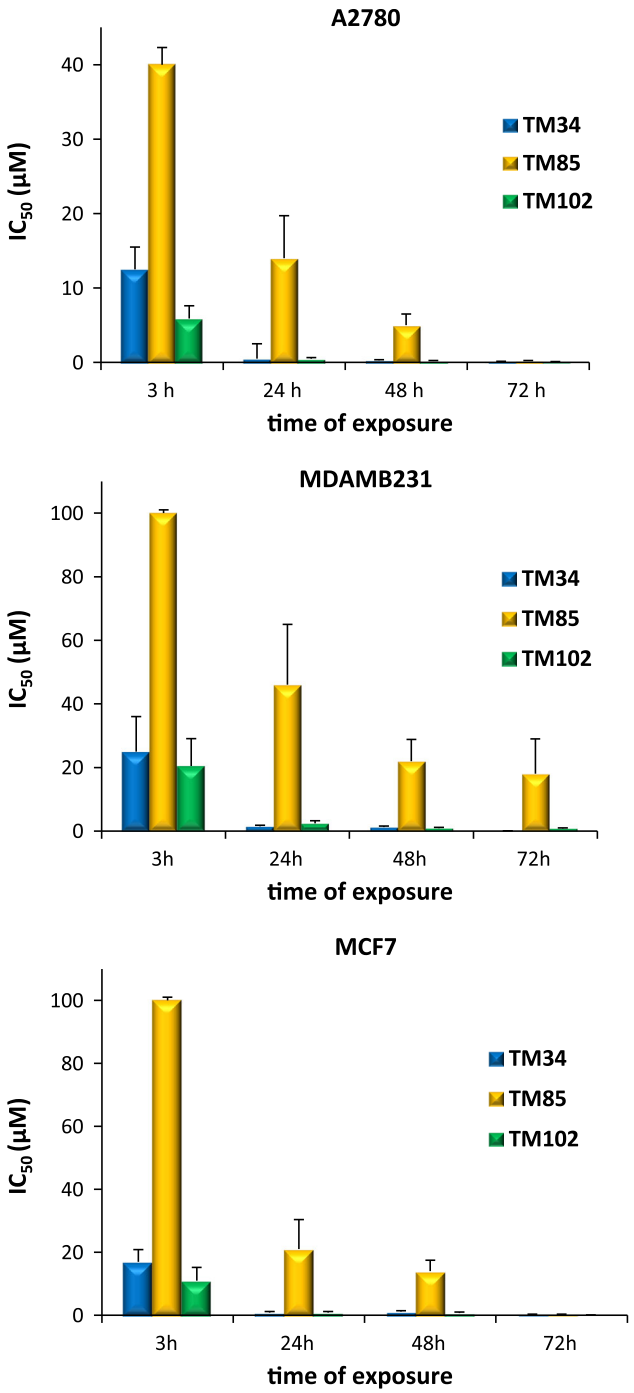

Fig. 2 Half-maximal inhibitory concentrations (IC_{50}) found for TM34, TM85, and TM102 in A2780, MDA-MB-231, and MCF7 cells at different exposure times. The results are expressed as mean values (± the standard deviation, SD) of three independent experiments with at least six replicates

The effects of the complexes on the cellular viability determined by AcP and NR assays were evaluated in MDA-MB-231 cells after 3 h exposure to the complexes at 1, 10, and 100 μM. The results depicted in Fig. 3 allowed a comparison between assays regarding differences in the sensitivity. NR cytotoxicity assay, which measures the uptake of compounds by the functional lysosomes, was the less sensitive except for higher concentration of the complexes (TM34 and TM102, 100 μM). Curiously, AcP assay seemed the most sensitive method, revealing loss of viability following exposure to the complexes before any cytotoxicity was observed when the MTT assay or NR assay was used.

Cytotoxicity with complex–transferrin conjugates

Serum proteins play a crucial role in the transport and delivery of drugs and may be involved in the mechanism of action of antitumor metallodrugs [65]. Interactions with blood carrier proteins can affect the drug biological activity and cytotoxicity [23].

In this context, experiments were undertaken to evaluate if the binding of complexes to human transferrin could influence their cytotoxic activity in A2780 cells in comparison with the complexes alone. As can be observed from Fig. 4, cellular viability increased by approximately 10–15 % in the presence of transferrin alone. However, when bound to transferrin, the complexes preserve their cytotoxic activity.

DNA interaction

We also evaluated the reactivity of TM34, TM85, and TM102 with DNA, the main target of cisplatin. DNA damage induced by the ruthenium complexes and cisplatin was studied in vitro by monitoring the drug-induced conformational change of supercoiled ΦX174 plasmid DNA. Closed circular, supercoiled DNA was treated at 37 °C for 24 h in phosphate buffer (pH 7.2) with various concentrations of the ruthenium complexes or cisplatin. The dose-dependent conformational changes of the treated DNA were detected by agarose gel electrophoresis.

As shown in Fig. 5, the electrophoretic mobilities of both the nicked and the closed circular DNAs change after incubation with cisplatin, but not after incubation with the ruthenium complexes. For the former metallodrug, the mobility of the nicked DNA band (form II) increases with increased platinum binding. This indicates the shortening of the DNA helix, as cisplatin will produce a more compact DNA structure on binding. Even more substantial are the changes in the electrophoretic mobility of the supercoiled DNA with platinum binding, due to localized unwinding of the duplex DNA [66, 67]. We can conclude that the ruthenium complexes, in contrast to cisplatin, do not affect the mobility of DNA, indicating no formation of adducts. This seems to indicate that the DNA double helix is not a primordial target of these ruthenium complexes.

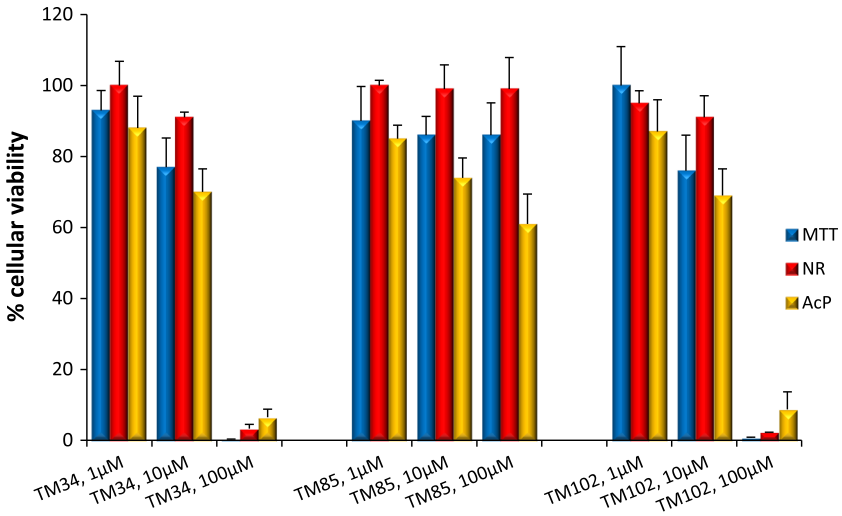

Fig. 3 Comparison of 3-(4,5-dimethyl-2-thiazolyl)-2,5-diphenyltetrazolium bromide (*MTT*), neutral red (*NR*), and acid phosphatase (*AcP*) assays in MDA-MB-231 cells after 3 h exposure to the complexes at 1, 10, and 100 μM. The results are expressed as mean values (± SD) of two independent experiments with at least six replicates

Cellular distribution of ruthenium complexes determined by ICP-MS

The cellular distribution of the complexes, measured as ruthenium accumulation, was determined to relate the uptake with the cytotoxic activities displayed. The ruthenium content in cytosol, membrane/particulate, nuclei, and cytoskeletal fractions isolated from cells after 3 h of exposure to the complexes at 10 μM was determined by ICP-MS, and the results are shown in Fig. 6. For comparison, cisplatin was included in this study using the same experimental protocol, 3 h of exposure to the drug at 10 μM with the A2780 ovarian cells (cisplatin-sensitive), and the content of platinum is also presented. The equimolar concentration of 10 μM was selected in order to make comparisons for the same concentration differences in the uptake of the complexes.

As can be observed from Fig. 6, the ruthenium complexes TM34 and TM102 present a very similar profile, i.e., preferential localization at the membranes (70–80 % of total Ru) and negligible ruthenium content in the nucleus [24]. Compared with TM34, TM102 showed a slightly higher cellular accumulation: 4.42 nmol Ru/mg protein versus 3.78 nmol Ru/mg protein (about 14 %). The accumulation of TM85 is much lower than that of its congeners but presents a quite similar profile, i.e., a higher amount of ruthenium is localized in the membranes but also in cytoskeleton fractions, both fractions representing more than 90 % of total ruthenium taken up by the cells. In addition, the distribution of the complexes in the individual fractions has a profile different from that for cisplatin. For cisplatin, platinum is predominantly localized in the cytosol and nucleus (approximately 75 %). The results from this study in A2780 cells indicate a relationship between accumulation and cytotoxicity, i.e., the water-soluble "version" of TM34 although gaining solubility seemed to lose activity. Moreover, the complexes can interact with components, proteins, and other biomolecules present in the membranes/cytoskeleton, thus representing their potential targets.

We also performed ICP-MS of samples of cellular suspensions and determined the total ruthenium content using for each complex a concentration equivalent to the IC_{50} values found for complexes after 3 h treatment. The results from this study (Table 2) indicated a very low uptake of TM85 even at high concentrations (40 μM).

Cellular uptake of complex–transferrin conjugates

The amount of ruthenium taken up by A2780 cells after binding of the complex to transferrin was quantified by ICP-MS. The experimental conditions were as described in "Cellular viability assays with complex–transferrin conjugates." The results presented in Fig. 7 showed for TM34 and TM85 an increase in accumulation of the complex when its was conjugated to transferrin: for TM34, 1.15 nmol Ru/mg protein versus1.82 nmol Ru/mg protein, and for TM85, 0.08 nmol Ru/mg protein versus 0.13 nmol Ru/mg protein, which represent an uptake 1.6–1.7 times higher than that observed for the free ruthenium complexes. Inversely, the uptake of TM102 when conjugated to transferrin declined when compared with that of the unbound compound. The results suggest that for TM34 and TM85, the binding to transferrin facilitates entry into the cells and in addition does not alter their efficacy.

The results from this study indicated, like those presented in Table 2 (analysis of ruthenium in cellular suspensions), a similar trend. It is interesting that at 24 h the ruthenium content is lower than what was observed at 3 h (Table 2, Fig. 7).

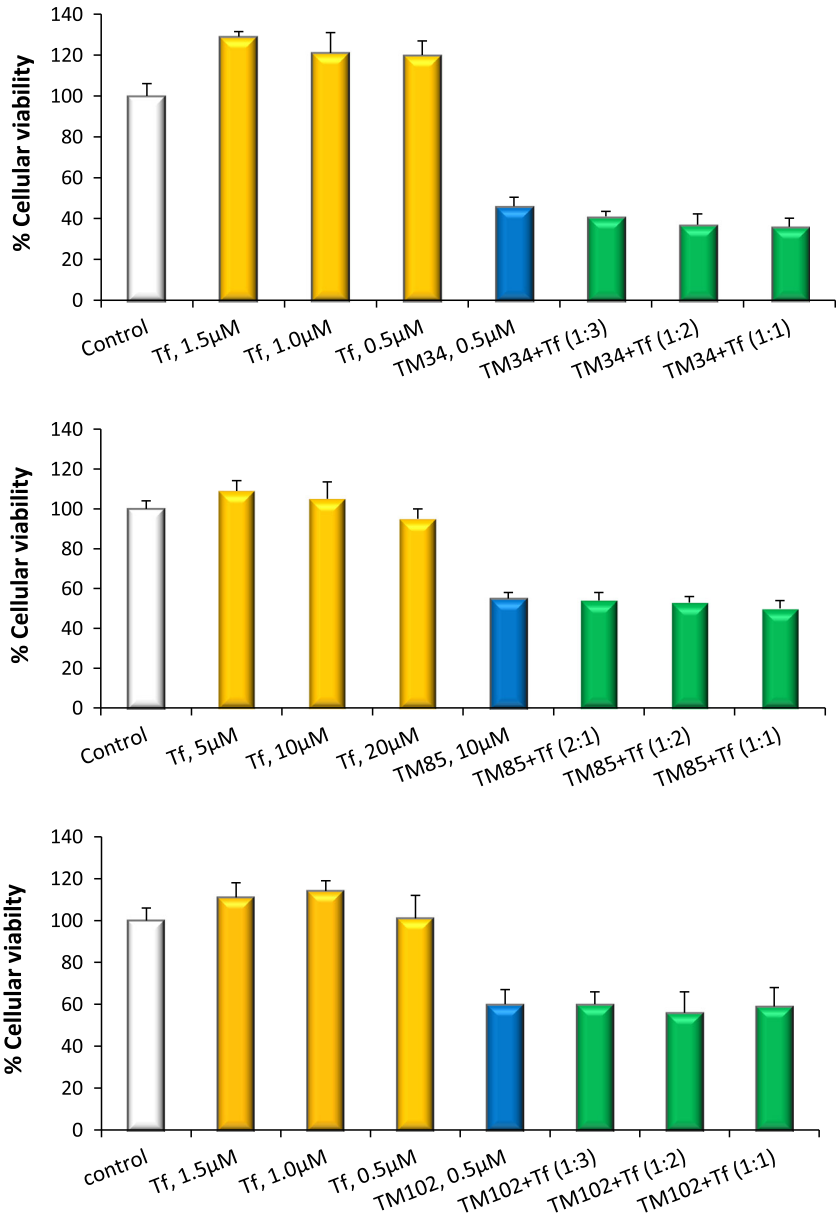

Fig. 4 Effect of transferrin (*Tf*) on the cytotoxicity of complexes toward A2780 cells after a 24-h challenge with different complex-to-protein molar ratios. The data shown represent cells with no treatment (negative control), cells treated with Tf alone at concentrations used for conjugation of the complex, and cells treated with complex–Tf conjugates. The results are expressed as mean values (± SD) of two independent experiments with at least six replicates

Metabolism and lactic acid levels

The amount of lactic acid produced by malignant cells is directly proportional to the aggressiveness of the cancer, as the glycolytic metabolism is modified and enhanced, allowing cellular proliferation. According to the Warburg hypothesis, aggressive cancers obtain much of their ATP by metabolizing glucose directly to lactic acid [35]. MDA-MB-231 cells have a high glycolytic rate because of their aggressive phenotype and invasive behavior.

The lactate levels were determined using a colorimetric assay, in which lactate is oxidized to pyruvate by lactate dehydrogenase to generate a product which interacts with a probe to produce a colored compound ($\lambda_{max} = 570$ nm). MDA-MB-231 cells exhibited an altered glycolytic metabolism, producing higher levels of lactate compared with MCF7 cells (18 μM vs 3 μM). The effect of the glycolytic inhibitors 2DG, 3BrP, and DCA was studied because they are currently used in preclinical development or clinical therapies. The pharmacological action of these drugs is based on ATP depletion and inhibition of pyruvate production. Figure 8 shows the effect of these glycolytic inhibitors when studied at noncytotoxic concentrations. 2DG, a recognized lactate inhibitor, can have a role as a positive control for this experiment. At 20 mM, it inhibits to a great extent the production of lactate (about 75 % relative to controls). The complexes at 5 μM (TM34,

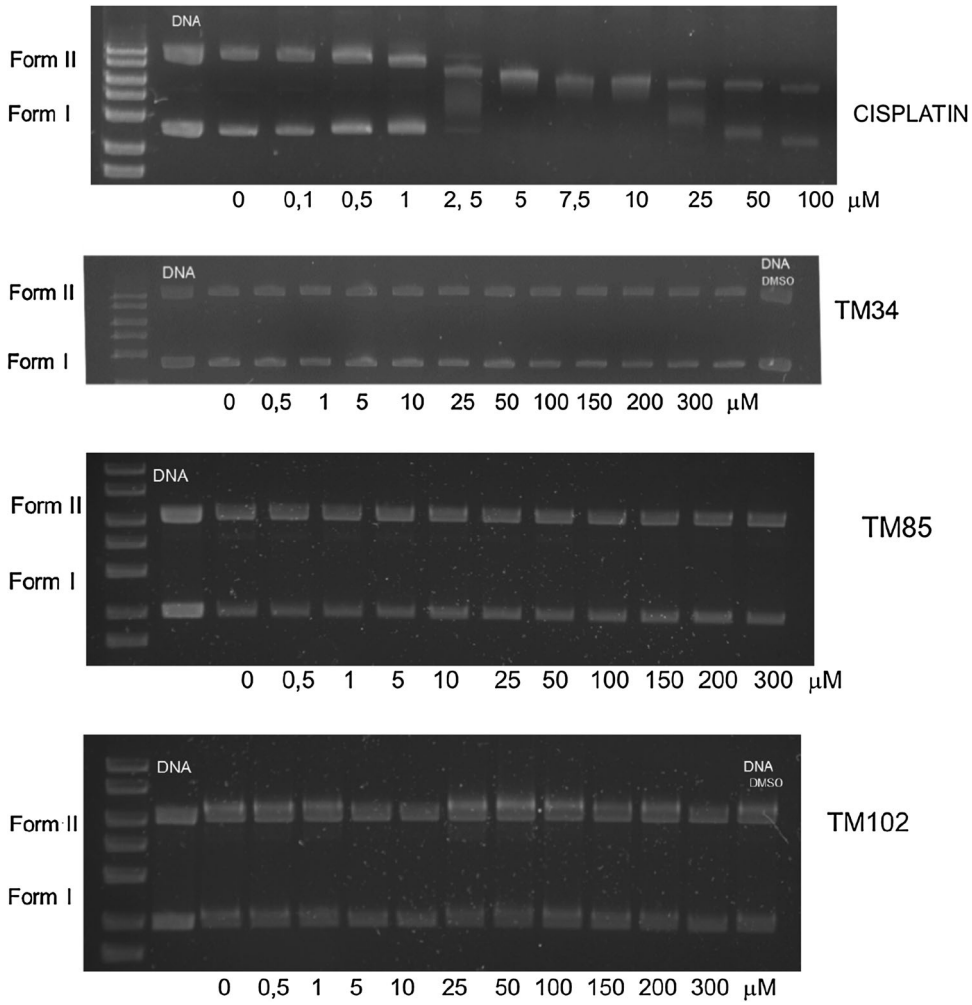

Fig. 5 Interaction between supercoiled ΦX174 plasmid DNA and cisplatin and ruthenium complexes TM34, TM85, and TM102, after 24 h incubation at 37 °C in phosphate buffer (pH 7.2). Forms I and II are supercoiled and nicked circular forms of DNA, respectively

TM102) and 100 µM (TM85) also induced an inhibitory effect on the production of lactate.

Effect of glycolytic inhibitors and their combination with the complexes on cellular viability

TM85 shows moderate cytotoxicity compared with its analogues, probably because of its water solubility owing to the presence of the soluble phosphine ligand. Taking into consideration that this property may have advantages if we consider its use for clinical applications, we studied the effect of the glycolytic inhibitors 2DG, 3BrP, and DCA combined with TM85 in order to evidence a possible potentiation of its antiproliferative activity. 2DG, 3BrP, and DCA were tested at a concentration that did not induce a cytotoxic effect but instead inhibited aerobic glycolysis (lactate production).

Figure 9 shows the effect of the inhibitors combined with TM85 on the MDA-MB-231 cellular viability by the MTT assay. 2DG, 3BrP, and DCA cause ATP depletion, although they act at different steps in glycolysis: (1) 2DG enters cells via glucose transporters and inhibits hexokinase; (2) 3BrP enters cells via lactic acid transporters and owing to its alkylating properties inhibits both pyruvate kinase and glyceraldehyde 3-phosphate dehydrogenase; (3) DCA enters cells probably by sodium-coupled monocarboxylate transporters and inhibits mitochondrial pyruvate dehydrogenase kinase [68].

As shown in Fig. 9, the combination of ruthenium with the glycolytic inhibitors led to a massive loss of cell viability. We expected to observe a higher cytotoxic effect of 3BrP combined with the complex. Nevertheless, 2DG and DCA seemed to be the most promising compounds, acting even for lower concentrations of the complex.

Trans-plasma-membrane electron transport

Membrane-bound oxidoreductases are common to all living organisms. Some are structured plasma membrane integral proteins as TPMET systems [41–43].

The results obtained for the effect of the complexes and inhibitors on TPMET activity of MDA-MB-231 cells using

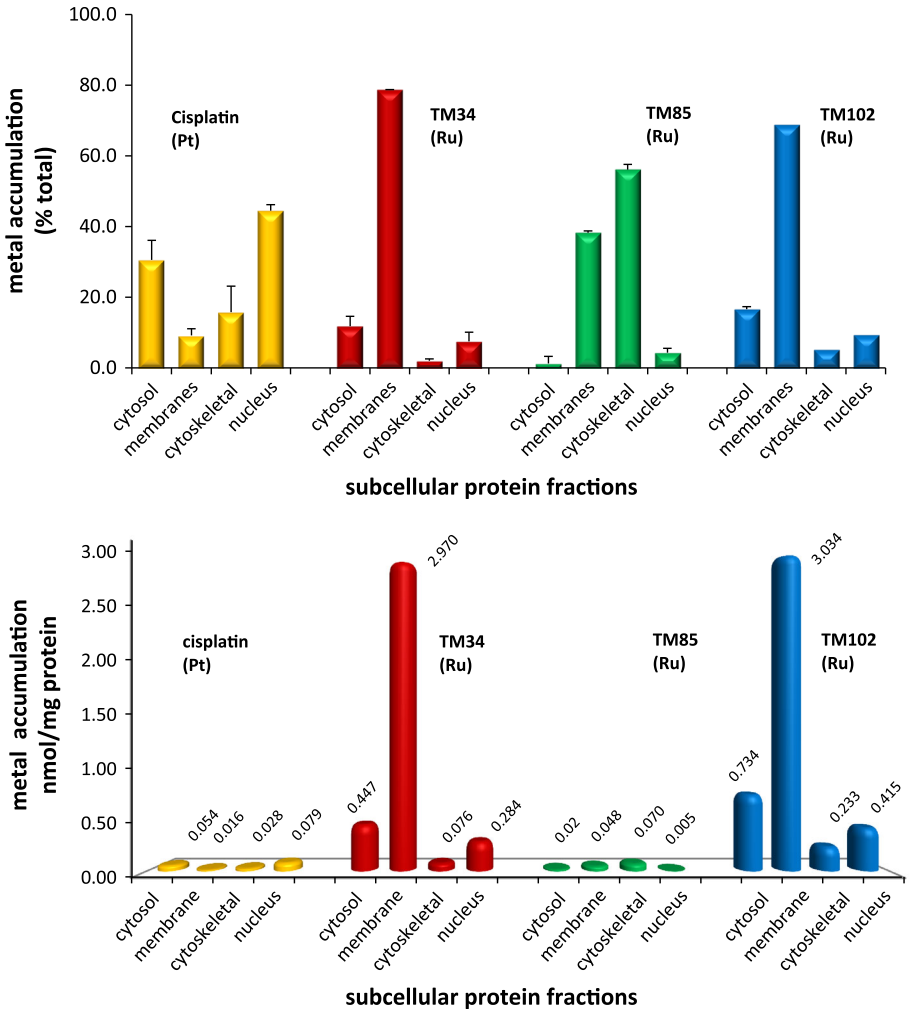

Fig. 6 Metal accumulation in the A2780 subcellular fractions after 3 h exposure to the complexes at an equimolar concentration of 10 μM. *Top*: Results expressed as a percentage of total metal accumulation. *Bottom*: Results expressed as nanomoles of ruthenium per milligram of protein or nanomoles of platinum per milligram of protein. Cisplatin was included as the reference metallodrug in clinical use

Table 2 Ruthenium content in A2780 cells extracts after 3 h exposure to the complexes at a concentration equivalent to the IC_{50} values

Complex	Ru content (nmol Ru/mg protein)
TM34 (12 μM)	2.04 ± 0.04
TM85 (40 μM)	0.02 ± 0.01
TM102 (6 μM)	1.30 ± 0.02

The results represent the mean ± the standard deviation of two independent experiments.

ferricyanide as the electron acceptor are presented in Table 3. All compounds were studied at concentrations that did not induce a cytotoxic response during the 30 min incubation. Enzyme activity was shown to be highly sensitive to thiol reagents. Inhibition by impermeable sulfhydryl reagents such as pCMBS and DTNB and permeable reagents such as PAO suggests that cysteine residues appear to be essential for the catalytic activity and are not solely located at the membrane. The results in Table 3 show that PAO (10 μM) and DTNB (10 μM) inhibit basal activities by approximately 70 and 80 %, respectively, and pCMBS totally abolishes reductase activity but at higher concentrations (1 mM).

The reductase enzyme is coupled to the Na^+/H^+ antiport. Blockade of the exchanger has been shown to inhibit NADH-ferricyanide reductase [69]. Amiloride, a Na^+/H^+ inhibitor, and chloroquine, a lysosomotropic drug, modulate transmembrane H^+ movement. Both drugs inhibit to similar extent and at a similar concentration the reductase activity (90–95 %, 1 mM).

The enzyme is sensitive to compounds that interfere with glucose uptake and glycolysis, as 2DG, confirming the close connection between TPMET and this metabolic pathway [58].

The ruthenium complexes inhibit the enzyme at micromolar concentrations, in particular for TM34 and TM85. TM102 exhibits a high inhibitory effect at submicromolar concentrations. As can also be seen from Table 3, the precursors $Ru(\eta^5\text{-}C_5H_5)(PPh_3)_2Cl$ and $Ru(\eta^5\text{-}C_5H_5)(\text{-}mTPPMSNa)_2Cl$) have a lower inhibitory effect compared with the complexes. Cisplatin was introduced as a control exhibiting a very similar inhibitory effect to that of TM34,

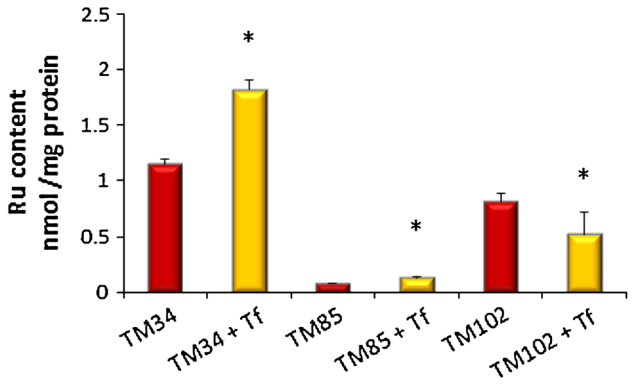

Fig. 7 Ruthenium content in A2780 cell extracts after 24 h exposure to the complexes at 0.5 μM (TM34), 10 μM (TM85), and 0.5 μM (TM102) and 1:2 metal-to-protein molar ratios. The results represent the mean ± SD of two independent experiments. *Asterisk* $P < 0.05$ versus the complex alone

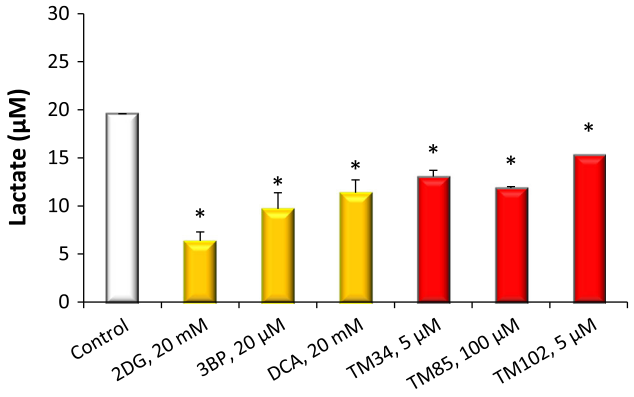

Fig. 8 Effect of glycolytic inhibitors—2-deoxyglucose (*2DG*), 3-bromopyruvate (*3BP*), and dichloroacetate (*DCA*)—and the complexes on lactate levels of MDA-MB-231 cells after 3 h exposure to the compounds. The results are expressed as the mean ± SD of two independent experiments with at least six replicate runs. *Asterisk* $P < 0.05$ versus the control

i.e., 80 % inhibition at 10 μM. The cisplatin inhibitory effect is thought to be mediated through the coordination to sulfur atoms of glycolytic enzymes [25, 59].

Discussion

Platinum-based anticancer drugs, such as cisplatin, have been widely used to treat a variety of cancers, although they have several limitations related to toxicity and resistance. The primary target for platinum drugs is DNA. However, recent developments in biomedical research have identified several other targets for cisplatin.

Active glycolysis in cancer cells suggests a possibility to preferentially inhibit cancer cell metabolism by targeting glycolytic enzymes and glycolysis regulators. Cisplatin targets glycolysis by inhibiting aldolase and glyceraldehyde 3-phosphate dehydrogenase probably through the coordination to the sulfur atoms of the enzymes [25].

Ruthenium drugs are believed to act on tumors through mechanisms of action different from those attributed to cisplatin and have the advantage of being less toxic or even overcoming the problems of resistance. These compounds represent new and efficient therapeutic drugs as alternatives to platinum-based drugs and are currently being evaluated for pharmacological applications.

Here we have highlighted a series of related Ru(η^5-C_5H_5) complexes—TM34, TM85, and TM102–with important antitumor activity in a set of tumor cell lines—A2780 (ovarian) and MCF7 and MDA-MB-231 (breast)—and have illustrated their properties as prospective anticancer drugs. TM34, TM85, and TM102 enter cells and inhibit cell growth. When they are conjugated with transferrin, uptake is facilitated (A2780: TM34, TM85) and no loss of activity was observed when the complexes bound to the blood carrier protein.

The results obtained from the cytotoxic assays indicate that there are differences between the three cell lines regarding their sensitivity to the complexes. A2780 cells appear to be more sensitive as indicated by the MTT assay. From previous results, the higher cytotoxic effect observed for TM34 in ovarian cancer cells could be explained by additional morphological alterations of the mitochondria, i.e., high densification of the matrix compared with breast cancer cells [24]. The cytotoxicity assays used revealed different profiles, with AcP assay being the most sensitive, which suggests a localized effect on the lysosomes before any significant effect on mitochondria.

Complex preferential localization at the cell membrane in addition to no observable interaction with DNA prompted us to identify other possible targets at the cell membrane. TPMET systems have been extensively documented as ubiquitous in all cells, acting as redox regulators of cellular metabolism. TPMET is inhibited by anticancer drugs at concentrations which correlate with their cytotoxic effect [12, 59].

TPMET has been demonstrated using artificial cell-impermeable substrates such as ferricyanide, 2,6-dichlorophenolindophenol, and 2-(4-iodophenyl)-3-(4-nitrophenyl)-5-(2,4-disulfophenyl)-2*H*-tetrazolium sodium salt. The presence of an intermediate electron carrier (1-methoxy-5-methylphenazinium methyl sulfate) was obligatory for 2-(4-iodophenyl)-3-(4-nitrophenyl)-5-(2,4-disulfophenyl)-2*H*-tetrazolium sodium salt reduction, whereas ferricyanide and 2,6-dichlorophenolindophenol are reduced directly. Reduction of all these substrates is not similarly altered by metabolic modulators, which indicates there are distinct TPMET pathways [70].

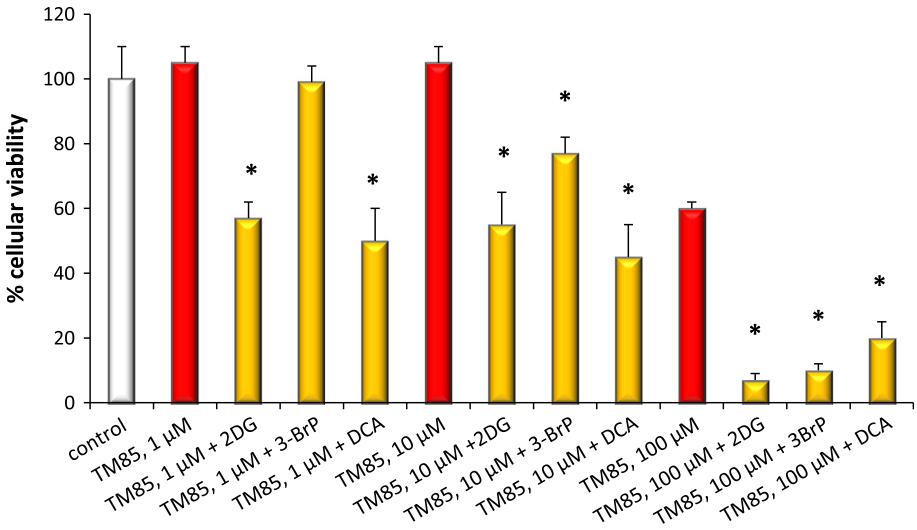

Fig. 9 Effect of glycolytic inhibitors—20 mM 2DG, 20 μM 3-bromopyruvate (*3-BrP*, *3BrP*), and 20 mM DCA—and their combinations with TM85 on MDA-MB-231 viability determined by the MTT assay after 24 h incubation. The results are expressed as the mean ± SD of two independent experiments with at least six replicate runs. *Asterisk* $P < 0.05$ versus the complex alone (at the corresponding concentration)

Table 3 Effect of the complexes and inhibitors on ferricyanide reduction

Compound	Ferrocyanide formation (% of control)
None (control)	100 ± 6.9
$RuCp(PPh_3)_2Cl$	62.4 ± 10
$RuCp(mTPPMSNa)_2Cl$	87.6 ± 6.7
TM34 (10 μM)	19.3 ± 1.0
TM85 (10 μM)	66.1 ± 0.63
TM102 (0.1 μM)	14.7 ± 0
pCMBS (1 mM)	0
2DG	33.6 ± 2.5
DTNB (10 μM)	25.9 ± 0
PAO (10 μM)	25.9 ± 0
Chloroquine (1 mM)	10.0 ± 1.1
Amiloride (1 mM)	5.07 ± 1.3
Cisplatin (10 μM)	20.7 ± 1.9

MDA-MB-231 cells (approximately 1×10^6–1.5×10^6 cells) were preincubated for 15 min with the compounds. Then, 1 mM ferricyanide was added and the cells were incubated for an additional 15 min. At the end of the incubation, ferrocyanide was determined as described in "Measurement of TPMET." Ferrocyanide found for controls (no treatment): 44.8 ± 3.1 nmol/min mg protein. The results are the mean ± SD) of at least two independent experiments.

Cp η^5-C_5H_5, *2DG* 2-deoxyglucose, *DTNB* dithionitrobenzoic acid, *mTPPMS* *m*-diphenylphosphane benzene-3-sulfonate *PAO* phenylarsine oxide, *pCMBS* *p*-chloromercuribenzene sulfonate, PPh_3 triphenylphosphane

On the basis of previous results obtained by us [45–47, 49] that demonstrate the presence of a plasma membrane redox system in human erythrocytes related to glycolytic pathways and implicated in redox regulation and erythrocyte metabolism, we decided to demonstrate with the MDA-MB-231 cells, which are known for their high glycolytic phenotype, the presence of this redox enzyme together with the potential of the ruthenium complexes to inhibit this system. In this decision we took into consideration what was found for some antitumor drugs, particularly cisplatin, that target glycolysis by inhibiting glycolytic enzymes and NADH-ferricyanide reductase activity.

In our study TPMET was demonstrated in MDA-MB-231 breast cancer cells using the cell-impermeable substrate ferricyanide. The enzyme was sensitive to sulfhydryl reagents, metabolic inhibitors, pH change related to proton efflux, and the ruthenium complexes. An interesting finding was that the complexes inhibit the reductase enzyme in a mode apparently related to their cytotoxic potential. Similarly, lactate levels were also inhibited by the complexes in a way related to their cytotoxic activity.

TM85 was the least active complex in all cells studied. Even so, the cytotoxic effect in A2780 cells was superior to that observed for cisplatin under the same experimental conditions after 72 h treatment (0.21 ± 0.04 μM vs 1.9 ± 0.10 μM) [21]. By ICP-MS, we found the distribution profile in A2780 cells is completely different from that observed for cisplatin, i.e., preferential accumulation of the complex in the membranes and cytoskeleton. Certainly, this was an interesting finding regarding the role of the cytoskeleton in the cell proliferation process and cancer development. Because a number of commonly used cancer drugs inhibit cell proliferation by disrupting cytoskeletal function, the cytoskeleton may have a broad potential for drug discovery and development [71].

The effect of the glycolysis inhibitors 2DG, 3BrP, and DCA in combination with TM85 on the cytotoxic activity of TM85 was studied. We demonstrated that all inhibitors synergized with TM85 induced cytotoxicity. This combination of compounds was more efficient than either

compound alone. The results indicate that targeting cellular metabolism can improve the response to cancer therapeutics. The combination of chemotherapeutic drugs with metabolic inhibitors may represent a promising strategy to overcome drug resistance, thus creating new strategies for cancer therapy [72].

Acknowledgments This work was financed by national funds through FCT, the Portuguese Foundation for Science and Technology, within the scope of projects PTDC/QUI-QUI/101187/2008, PTDC/QUI-QUI/118077/2010, PEst-OE/QUI/UI0100/2011, and PEst-OE/QUI/UI0536/2011, as well as the Ciência2007 initiative. T.S.M. thanks FCT for her PhD grant (SFRH/BD/45871/2008), and A.V. thanks FCT for her postdoctoral grant (SFRH/BPD/80459/2011).

References

1. Wang D, Lippard SJ (2005) Nat Rev Drug Discov 4:307–320
2. Zhang CX, Lippard SJ (2003) Curr Opin Chem Biol 7:481–499
3. Reedijk J (2009) Eur J Inorg Chem 2009:1303–1312
4. Klein AV, Hambley TW (2009) Chem Rev 109:4911–4920
5. Hartinger CG, Zorbas-Seifried S, Jakupec MA, Kynast B, Zorbas H, Keppler BK (2006) J Inorg Biochem 100:891–904
6. Groessl M, Reisner E, Hartinger CG, Eichinger R, Semenova O, Timerbaev AR, Jakupec MA, Arion VB, Keppler BK (2007) J Med Chem 50:2185–2193
7. Hartinger CG, Jakupec MA, Zorbas-Seifried S, Groessl M, Egger A, Berger W, Zorbas H, Dyson PJ, Keppler BK (2008) Chem Biodivers 5:2140–2155
8. Peacock F, Sadler PJ (2008) Chem Asian J 13:1890–1899
9. Levina A, Mitra PA (2009) Metallomics 1:458–470
10. Bergamo A, Masi A, Peacock AF, Habtemariam A, Sadler PJ, Sava G (2010) J Inorg Biochem 104:79–86
11. Bergamo A, Gaiddon C, Schellens JH, Beijnen JH, Sava G (2012) J Inorg Biochem 106:90–99
12. Sancho-Martínez SM, Prieto-García L, Prieto M, López-Novoa JM, López-Hernández FJ (2012) Pharmacol Ther 136:35–55
13. Jakupec MA, Galanski M, Arion VB, Hartinger CG, Keppler BK (2008) Dalton Trans 183–194
14. Brabec V, Nováková O (2006) Drug Resist Updates 9:111–122
15. Casini A, Gabbiani C, Sorrentino F, Rigobello MP, Bindoli A, Geldbach TJ, Marrone A, Re N, Hartinger CG, Dyson PJ, Messori L (2008) J Med Chem 51:6773–6781
16. Bruijnincx PC, Sadler PJ (2008) Curr Opin Chem Biol 12:197–206
17. Mura P, Camalli M, Casini A, Gabbiani C, Messori LJ (2010) J Inorg Biochem 104:111–117
18. Fricker SP, Ciancetta A, Genheden S, Ryde UJ (2011) J Comput Aided Mol Des 25:729–742
19. Moreno V, Font-Bardia M, Calvet T, Lorenzo J, Avilés FX, Garcia MH, Morais TS, Valente A, Robalo MP (2011) J Inorg Biochem 105:241–249
20. Morais TS, Silva TJ, Marques F, Robalo MP, Avecilla F, Madeira PJ, Mendes PJ, Santos I, Garcia MH (2012) J Inorg Biochem 114:65–74
21. Morais TS, Santos FC, Jorge TF, Côrte-Real L, Madeira PJA, Marques F, Robalo MP, Matos A, Santos I, Garcia MH (2014) J Inorg Biochem 130:1–14
22. Morais TS, Santos F, Côrte-Real L, Marques F, Robalo MP, Madeira PJA, Garcia MH (2013) J Inorg Biochem 122:8–17
23. Tomaz AI, Jakusch T, Morais TS, Marques F, Almeida RF, Mendes F, Enyedy EA, Santos I, Pessoa JC, Kiss T, Garcia MH (2012) J Inorg Biochem 117:261–269
24. Côrte-Real L, Matos AP, Alho I, Morais TS, Tomaz AI, Garcia MH, Santos I, Bicho MP, Marques F (2013) Microsc Microanal 24:1–9
25. Pedersen PL (2007) J Bioenerg Biomembr 39:1–12
26. Moreno-Sánchez R, Rodríguez-Enríquez S, Marín-Hernández A, Saavedra E (2007) FEBS J 274:1393–1418
27. Rodríguez-Enríquez S, Marín-Hernández A, Gallardo-Pérez JC, Carreño-Fuentes L, Moreno-Sánchez R (2009) Mol Nutr Food Res 53:29–48
28. Gatenby RA, Gillies RJ (2007) Int J Biochem Cell Biol 39:1358–1366
29. Warburgh O (1956) Science 124:269–270
30. Hirschhaeuser F, Sattler UG, Mueller-Klieser W (2011) Cancer Res 71:6921–6925
31. DeBerardinis RJ (2008) Genet Med 10:767–777
32. Bartrons R, Caro J (2007) J Bioenerg Biomembr 39:223–229
33. Scatena R, Bottoni P, Pontoglio A, Mastrototaro L, Giardina B (2008) Expert Opin Investig Drugs 17:1533–1545
34. Zhang F, Aft RL (2009) J Cancer Res Ther 5:41–43
35. Mathupala SP (2011) Recent Pat Anticancer Drug Discov 6:6–14
36. Pedersen PL (2012) J Bioenerg Biomembr 44:1–6
37. Shoshan MC (2012) J Bioenerg Biomembr 44:7–15
38. Cardaci S, Desideri E, Ciriolo MR (2012) J Bioenerg Biomembr 44:17–29
39. Michelakis ED, Webster L, Mackey JR (2008) Br J Cancer 99:989–994
40. Sutendra G, Michelakis ED (2013) Front Oncol 3:1–11
41. Goldenberg H (1982) Biochim Biophys Acta 694:203–223
42. Lane DJ, Lawen A (2008) Biofactors 34:191–200
43. Löw H, Crane FL, Morré JD (2012) Int J Biochem Cell Biol 44:1834–1838
44. Del Principe D, Avigliano L, Savini I, Catani MV (2011) Anti-oxid Redox Signal 14:2289–2318
45. Marques F, Crespo ME, Bicho M (1995) Redox Rep 1:113–117
46. Marques F, Bicho MP (1997) Biol Signals 6:52–61
47. Marques F, Crespo ME, Silva ZI, Bicho M (1999) Protoplasma 206:168–173
48. Schipfer W, Neophytou B, Trobisch R, Groiss O, Goldenberg H (1985) Int J Biochem 17:819–823
49. Marques F, Crespo ME, Silva ZI, Bicho M (2000) Diabetes Res Clin Pract 47:191–198
50. Herst PM, Berridge MV (2007) Biochim Biophys Acta 1767:170–177
51. Orringer EP, Roer ME (1979) J Clin Invest 63:53–58
52. Baker MA, Lane DJ, Ly JD, De Pinto V, Lawen A (2004) J Biol Chem 279:4811–4819
53. Lane DJR, Lawen A (2008) Anal Biochem 373:287–295
54. Avron M, Shavit N (1963) Anal Biochem 6:549–554
55. Pieroni L, Khalil L, Charlotte F, Poynard T, Piton A, Hainque B, Imbert-Bismut F (2001) Clin Chem 47:2059–2061
56. Rodríguez-Alonso J, Montañez R, Rodríguez-Caso L, Ángel Medina M (2008) J Bioenerg Biomembr 40:45–51
57. Herst PM, Berridge MV (2006) Curr Mol Med 6:895–904
58. Prata C, Grasso C, Loizzo S, Vieceli Dalla Sega F, Caliceti C, Zambonin L, Fiorentini D, Hakim G, Berridge MV, Landia L (2010) Leuk Res. doi:10.1016/j.leukres.2010.02.032
59. Sun IL, Crane FL (1984) Biochem Int 9:299–306
60. Kim C, Crane FL, Faulk WP, Morré J (2002) J Biol Chem 277:16441–16447
61. Matos CP, Valente A, Marques F, Adão P, Robalo MP, Almeida RFM, Pessoa JC, Santos I, Garcia MH, Tomaz AI (2013) Inorg Chim Acta 394:616–626
62. Gama S, Mendes F, Esteves T, Marques F, Matos A, Rino J, Coimbra J, Ravera M, Gabano E, Santos I, Paulo A (2012) ChemBioChem 13:2352–2362
63. Fotakis G, Timbrell JA (2006) Toxicol Lett 160:171–177

64. Yang TT, Sinai P, Kain SR (1996) Anal Biochem 241: 103–108
65. Timerbaev AR, Hartinger CG, Aleksenko SS, Keppler BK (2006) Chem Rev 106:2224–2248
66. Cohen GL, Bauer WR, Barton JK, Lippard SJ (1979) Science 203:1014–1016
67. Bowler BE, Hollis LS, Lippard SJ (1984) J Am Chem Soc 106:6102–6104
68. Babu E, Ramachandran S, Kandaswamy VC, Elangovan S, Prasad PD, Ganapathy V, Thangaraju M (2011) Oncogene 30:4026–4037
69. Lane DJR, Robinson SR, Czerwinska H, Lawen A (2010) Biochem J 428:191–200
70. Tan AS, Berridge MV (2004) Redox Rep 9:302–306
71. Alberti C (2009) Eur Rev Med Pharmacol Sci 13:13–21
72. Ganapathy-Kanniappan S, Geschwind JFH (2013) Mol Cancer 12:152